

**TURBULENCE CHARACTERISTICS IN SUBMERGED  
HYDRAULIC JUMP BELOW SILLED SLUICE GATES BESIDES STUDYING ALSO THE  
SCALE EFFECTS IN FREE EFFLUX BELOW GATE OF VARIABLE OPENINGS**

**خصائص الاضطراب لقفزة هيدروليكية مغمورة خلف بوابات مزودة بأعتاب  
مع دراسة مدى تغير التصرف الحر خلف بوابة متغيرة الفتحات**

(1) M.I.ATTIA

*Assoe. Prof. water & water structures Engg. Dept.*

*Faculty of Engg. Zagazig University*

(2) IBRAHIM, M.H. RASHWAN

*Assoe. Prof. ,Civil Engg. Dept. ,*

*Faculty of Engg. , Kafrelsheikh University, Egypt*

**ملخص:** يتناول هذا البحث دراسة خصائص الجريان المضطرب للقفزات الهيدروليكية المغمورة خلف البوابات ذات الأعتاب باستخدام جهاز الليزر الحديث (LDV) في القنوات المستطيلة الأفقية وذلك لنسب غمر مختلفة من (0.2-1.5) ولقيم مختلفة لعدد فراود في المدخل  $F_{r1}$  (3-8) استخدم في هذا البحث عتب على شكل شبه منحرف ذات ميل 1:1 في الأمام والخلف حيث أثبتت الدراسات السابقة أن أفضل عتب على شكل شبه منحرف يمكن استخدامه لتحسين خصائص الجريان الحر والمغمور. ولهذا الغرض أجريت الدراسة العملية لقياس كثافات الاضطراب ومقاومة الاضطراب والسرعات المتوسطة في الإتجاهات المختلفة في اتجاه السريان والإتجاهات العمودية عليه وذلك لقطاعات عرضية مختلفة خلف البوابات في حالات القفزات الهيدروليكية المغمورة وبعدها. كذلك تم دراسة تأثير فتحة البوابات على خصائص السريان المختلفة وذلك لقيم مختلفة للإرتفاع النسبي  $Y_1/h_1$  وهي 0.1 ، 0.2 ، 0.3 ، 0.4 ، 0.5 ، 0.6 وتم عمل منحنيات لابعديه توضح كثافات الاضطراب ومقاومة قص الاضطراب والسرعات في الإتجاهات المختلفة ودراسة مقارنة لهذه المتغيرات عند القطاعات العرضية المختلفة داخل القفزة الهيدروليكية وبعدها كذلك تمت دراسة المقارنة للمتغيرات عند عدة مواضع مختلفة للعرض النسبي  $z/B$  عند نفس القطاع. وقد تبين من تحليل البيانات ومناقشة النتائج أن معامل التصرف للبوابات يتوقف على معامل الاتضغاط ومعامل الفقد في الطاقة كما يتأثر بمتغيرات الجريان ومتغيرات العتب وكذلك حالة الجريان وبالتالي معامل التصرف ذاته.

**ABSTRACT:**

In the present research , an experimental set up was arranged to investigate the scale effects in the free efflux below the sluice gate of variable openings and also to study the turbulence structure in the generated submerged hydraulic jump below the silled gate . The objective of the present study research was is to analyze the collected experimental data on the effect of constructing a sill under a sluice gate on the free and submerged flow bellow it . Also , this paper presents the results of a laser Doppler Anemometry (LDA) study of submerged hydraulic jumps in a horizontal rectangular channel with the different submergence factor  $S$  and different inlet Froude number  $F_{r1}$  . Measurements include surface profiles , mean velocity components of  $\bar{u}$  and  $\bar{v}$  ; turbulence intensities  $\bar{u}'$  and  $\bar{v}'$  and turbulence shear stress-  $\bar{u}'\bar{v}'$  . Major flow characteristics of submerged hydraulic jumps were discussed and analyzed . The flow in the fully developed region is found to have some degree of similarity . It was also found that a submerged jump was three dimensional in nature . The maximum vertical velocity in the recirculating zone for all submerged jumps is about 7% of  $U_1$ . Also , the results show that the maximum streamwise velocity near the center plane was smaller than that near the side wall . The turbulence shear stress near the center is about 46 % higher than that near the side wall . After the jump the flow will recover into a two dimensional flow . The coefficient of discharge becomes smaller at constant opening ratio  $Y_1 / h_1$  . The results showed that there was a close relationship between the scale effects in the contraction coefficients and in the discharge coefficients . The energy dissipation in effluxes was also related to the scale effect in the discharge coefficients closely . The scale effects in the contraction coefficient and in the coefficients of energy loss which are the main factors composing the discharge coefficients showed the same trend as in the discharge coefficient.

## **1. INTRODUCTION :**

The sluice gates are used in irrigation works in open channels to control the flow discharge and to measure its rate, and to besides controlling the water level upstream. Flow through gates may be free or submerged according to the extent of the water depth downstream the gate relative to the gate opening. They may be used in prismatic or in non - prismatic channels. It is well known that notable scale effects occur in the discharge coefficients of free efflux from an underflow gate sill obtained by the small scale model. There were many past works on the discharge coefficient, quantitative characteristics of the scale effect on the coefficient have not been made clear. It is one of the reasons that the ranges of the hydraulic conditions and of the model scales used in each works are not enough to clarify the whole aspects of the effect. Both the free and submerged flow below sluice gates on horizontal level floors were studied extensively [1,8,9,12,13,14,15,24]. In many cases, the irrigation engineer has to select between a double / triple leaf gates or a single/double leaf gate with sill constructed below. The selection of designing gates with sill reduces the cost of the gate material as well as the construction costs and that for the lifting device, also the power requirements are minimized. The effect of constructing sills under sluice gates on the flow below was investigated, some of these studies dealt with the free flow, Ranja Raju and Visavadia [21], Ranja Raju [22]. While others dealt with the submerged flow, El- Saiad etal [4,5]. Other studies dealt with the effect of the gate or sill configuration on the flow below the gate. Also, regarding the free and submerged flow, some studies are available in the literature, Salama [23]. Generally, it was found that the sill under the gate increased the coefficient of discharge of the gate and such rate of increase depends on the configuration of both the sill and gate as well as on both the sill and flow parameters. Hydraulic jumps were studied extensively because of their importance as energy dissipators for hydraulic structures. Experimental investigations have been carried out on both the macroscopic and internal structure of the hydraulic jumps, but most of these studies were directed to the macroscopic features. Major contributions of this subject were reviewed by Rajaratnam [16] and more recently by Mc Corquodale[11]. The hot - wire study in an air model by Rouse, Siao Nagaratnam [20] in 1958

was the first attempt to obtain information of turbulence field in free hydraulic jumps. More than a decade later in 1972, Resch and Leutheusser [19] used the hot - film technique to make some limited observations on the turbulence in free hydraulic jumps in the actual water model. Both of these observations have been very valuable for the understanding and prediction of internal structure of hydraulic jumps. The experiments described in this research paper are concerned with submerged hydraulic jumps in a horizontal rectangular channel of constant width. The LDA study was conducted to provide detailed measurements of the mean velocity components, turbulence intensity components and shear stress, which could be used as basis to improve the prediction methods. If submerged hydraulic jumps are viewed as transitional phenomena between free jumps and wall jets. This research study would then also serve the purpose of comparing these three classes of flows. Such research study also examines the three dimensionality of submerged hydraulic jumps, its effects on the mean velocity and turbulence fields and, more importantly, its implication to the production models. Also, in this research study through the systematic experiments with several scale models, it is intended to make clear that the scale effects appeared in the discharge coefficient quantitatively, and to indicate the minimum model size without any scale effects, and moreover to clarify the hydraulic mechanism of the scale effects.

## **2. EXPERIMENTAL ARRANGEMENT :**

The submerged jumps were formed just below a vertical gate in a horizontal open channel 0.4m width, 0.5m deep and 9.5m long with glass wall 6 mm thick and steel plate bed. The water was supplied from a constant head tank to the flume at the desired discharge that is continuously monitored with an on - line orifice meter.

A tail vertical gate was provided at the downstream end of the flume to maintain a required water depth of channel flow. The water was finally collected in a sump tank where it was pumped back to the overhead tank by a 15 HP pump. Depth measurements were taken using a needle point gauge with a reading accuracy of  $\pm 0.1$  mm. Uniform flow conditions were reached using a carefully designed inlet tank. A downstream adjustable gate was used to regulate the tail water surface elevation. In any experiment

, the discharge change and the water level in the head tank were maintained constant so as to keep Froude number ( $F_r$ ) constant at the gate. In order to provide a relatively uniform stream at the gate, a special entrance device with curved lower section (a quarter of circle with 0.15 m radius) was fitted to the gate. This inlet condition nearly eliminates the flow contraction after the gate. By regulating the downstream level, different submergence conditions could be achieved for any given supercritical Froude number. The sill model was made from perspex sheets with upstream and downstream slopes of 1:1. The gate was located at the center of the flat top of the 3cm wide sill. The sill was tested with fixed height of sill 3cm. The experiments were made with several scale models where gate openings and channel width were varied. The gate opening were varied from 1 to 12 cm. The width of the channel were 10,20,30, and 40 cm. The tailgate was controlled to create free or submerged flow below the gate. After attaining the stability conditions (the upstream depth remain unchanged) the depth upstream and downstream the gate were measured. The discharge, the gate opening and the width were recorded. Different discharges, different gate openings and different widths were considered. Adopting the definitions, the inlet Froude number  $F_r$  is defined as  $U_1 / \sqrt{gY_1}$  and the submerged factor  $S$  is defined as  $(Y_1 - Y_2) / Y_2$ , where  $U_1$  and  $Y_1$  are respectively the velocity and water depth of the supercritical stream at the gate (see Fig.1),  $g$  is the gravitational acceleration,  $Y_2$  is the subcritical sequent depth of the free jump for  $U_1$  and  $Y_1$  as obtained by the Belanger equation and  $Y_t$  is the far downstream (or tail water) depth in the flume. Current investigation covers the experimental conditions with the submergence factor  $S$  varying approximately from 0.20 to 1.50 and inlet Froude number  $F_r$  approximately equals to 3 to 8. The upstream water depth  $h_1$  was measured at the upstream section about 20  $Y_1$  far from the gate.

**3. MEASURING INSTRUMENT:**

The experimental data were collected using the two color back - scatter LDA system. The laser was a 5W Argon - Ion laser with actual power of about 500 mW. The two laser beams, one blue (488 nm) and one green (514.5 nm), were focused at a measuring point from one side of the channel through an optical lens. The focal length lens was selected for best signal quality and excellent

spatial resolution. The nominal measuring probe volume of the intersecting beams was an ellipsoid with diameter 0.05 mm and length 0.65 mm. Counter processors were used to evaluate the Doppler frequencies / Subsequent computer analysis consisted of velocity bias averaging and outlier rejection. The number of samples taken at every point was 6000 bursts. This corresponded to a sample averaging time of about 100 seconds. Before acquiring the data, the LDA signal was checked for its regular Doppler burst that correspond to a particle passing through the measuring volume. For submerged hydraulic jumps with high inlet Froude number and low submergence, more air is entrained into the flow. When air bubbles are present, the data acquisition rate is low. So for a region with relatively high concentration of bubbles the sampling time is up to 300 seconds.

**4. THEORETICAL ANALYSIS:**

The free efflux from a sharp edged vertical gate on the horizontal open channel shown in Fig. 1 was chosen as the subject of the present research. Main physical parameters concerning the efflux phenomenon were as follows: Geometrical parameters, gate opening ( $Y_1$ ), channel width ( $B$ ) and upstream water depth ( $h_1$ ). Kinematical parameters, discharge ( $q$ ) and acceleration due to gravity ( $g$ ). Dynamical parameters, density ( $\rho$ ), dynamic viscosity ( $\mu$ ) and surface tension ( $\sigma$ ).

The discharge  $q$  is uniquely determined when the upstream water depth  $h_1$  is given under the condition that the other parameters remain the same. That is,  $h_1$  and  $q$  are combined with each other by a functional relationship. Then, in the dimensional analysis it is sufficient to consider only one of them as a characteristic parameter. Any quantitative property  $\Phi$  of an efflux phenomenon is related to the above parameters by a functional relationship.

$$\Phi_1 = f_1 (Y_1, B, h_1, g, \rho, \mu, \sigma) \dots\dots\dots(1)$$

If  $q$  is used as a parameter instead of  $h_1$

$$\Phi_2 = f_2 (Y_1, B, q, g, \rho, \mu, \sigma) \dots\dots\dots(2)$$

Using  $Y_1, g$  and  $\rho$  as the basic quantities, the  $\pi$ -theorem gives the following non - dimensional relationships corresponding to the above two equations

$$\Phi_3 = f_3 ( \frac{Y_1}{h_1}, \frac{Y_1}{B}, R_{e1}, W_{e1} ) \dots\dots\dots(3)$$

$$\Phi_4 = f_4 (F_r, \frac{Y_1}{B}, R_{e1}, W_{e1} ) \dots\dots\dots(4)$$

in which,

$$F_{r1} = [q/\sqrt{gY_1} \cdot Y_1^2] \quad , \quad R_{e1} = [\sqrt{gY_1} \cdot Y_1/(\mu/\rho)]$$

and  $W_{e1} = [\sqrt{gY_1}/\sqrt{(\sigma/Y_1 \cdot \rho)}] \quad \dots\dots(5)$

Consequently, it is understood that quantitative properties of the efflux phenomenon such as a discharge coefficient, a contraction coefficient and so on could be described in terms of the four non – dimensional parameters  $Y_1/h_1$  (or  $F_{r1}$ ),  $Y_1/B$ ,  $R_{e1}$  and  $W_{e1}$ . In explaining the efflux problem, the opening ratio  $Y_1/h_1$  is used as a more common parameter rather than the Froude number. So, in the following, we also use  $Y_1/h_1$  as the flow parameter. Two systems of efflux with different length scale (for example, model and prototype, small and large models) are dynamically similar each other when four parameters described above are the same in both systems. In such a case the scale effect does not occur. But, if the same fluid is used in both systems as in general hydraulic model tests, the strict dynamical similarity could be obtained. Because as is evident in eq (5),  $R_{e1}$  and  $W_{e1}$  change with model size. If the degree of the influence of viscosity and surface tension on the efflux phenomenon is different in each systems, these systems are no longer dynamically similar. Then the phenomena in each systems are different, that is, the scale effects will occur. Firstly, the scale effects in the discharge coefficient obtained experimentally by several scale models will be shown. In the experiment, the model size is expressed by gate opening  $Y_1$ . When the gate opening is changed, the parameters  $R_{e1}$  and  $W_{e1}$  change simultaneously as shown in Fig.2. Therefore, the scale effects observed in the experimental data must be considered to be the sum of the influence of the viscosity and the surface tension. Next, for the modeling of the efflux phenomenon, we will consider in what way each dynamical factors influence on the scale effect.

The experiments have been made with several scale models where gate opening and channel width were varied. The discharge coefficient  $C$  was obtained by the following equation.

$$C = q / B \cdot Y_1 \sqrt{2gh_1} \quad \dots\dots(6)$$

The characteristics of scale effect in the discharge coefficient have been made clear to some extent by the experimental works described above. However, the mechanism of scale effect is not yet known. Here, the more detailed hydraulic

study to clarify the mechanism of scale effect will be discussed later.

**5. SCALE EFFECT IN THE MAIN FACTORS COMPOSING DISCHARGE COEFFICIENT:**

The factors composing the discharge coefficient are obtained by solving the following two basic equations in the hydraulic analysis. The energy equation between section 1 and 2.

$$\lambda_1 h_1 + \frac{\alpha_1 \cdot V_1^2}{2g} = \lambda_2 C_c \cdot Y_1 + \frac{\alpha_2 \cdot V_2^2}{2g} + h_L \quad \dots\dots(7)$$

the continuity equation can be expressed as follows

$$q = Bh_1 v_1 = BC_c \cdot Y_1 \cdot V_2 \quad \dots\dots(8)$$

in which,

$h_i$  : water depth ( $i=1,2$ ), and subscripts of 1 and 2 mean upstream and downstream sections respectively (see Fig.1).

$V_i$  : mean velocity at section  $i$ .

$\alpha_i$  : energy correction coefficient of Coriolis at section  $i$ .

$\lambda_i$  : pressure distribution coefficient of Jager at section  $i$ .

$C_c$ : contraction coefficient.

$h_L$  : head loss between two sections

Introducing the head loss in the form of

$$h_L = k \frac{V_1^2}{2g} \quad \dots\dots(9)$$

the discharge is given by

$$Q = B \cdot Y_1 \cdot C_c \{ [(\lambda_1 - \lambda_2 \cdot Y_1 \cdot C_c / h_1)] / [\alpha_2 + k - \alpha_1 (Y_1 \cdot C_c / h_1)^2] \}^{0.5} \cdot \sqrt{2gh_1} \quad \dots\dots(10)$$

Comparing the above equation with equation (6), it is shown that the discharge coefficient is expressed in the terms of  $C_c$ ,  $\alpha_i$ ,  $\lambda_i$ ,  $k$ , in addition to  $Y_1/h_1$ .

In these factors,  $\alpha_i$  and  $\lambda_i$  are nearly constant if the influence of their change on the discharge coefficient is very small even if they change with the model scale. Then, here, we consider the scale effect in the contraction coefficient  $C_c$  and the coefficient of energy loss  $k$ .

**6. RESULTS AND DISCUSSION:**

The experimental data of the discharge coefficient for each gate opening (ie. for each model size) are shown in Fig. 3. In this figure, Frangmeier – Strelkoff's theoretical curve [2] and Henry's experimental curve [3] are also shown them together. The former is the obtained by the

two – dimensional potential flow theory considering strictly the influence of the gravity.

Observing the data in each model size (except  $Y_1 = 1.0$  cm), the influence of the channel width is not clear, and it is considered to be negligible even if it exists. Then, it seems to be quite all right to discard the parameter  $Y_1/B$  from the present problem. It is also shown that the coefficient becomes larger as the model size becomes smaller at constant opening ratio  $Y_1/h_1$ . This means that scale effects are observed in the coefficient. To make the characteristics of scale effect clear, the reprocessing of data for the change of discharge coefficients to model size with  $Y_1/h_1$  in Fig.4. The experimental values in this figure are the average values of data obtained for several channel widths. From this figure, the characteristics of the change of coefficient to model size is explained as follows: the coefficient for each opening ratio increases sharply as the model size becomes smaller, and it converges to a constant value with the increase of model size for each  $Y_1/h_1$ .

The minimum model size in which the scale effect is considered to be negligible becomes larger with the increase of opening ratio. The scale effect in the coefficients obtained by the model where the gate opening is larger than 6.0 cm seems to be very small for  $Y_1/h_1 < 0.5$ . In Fig.5, nearly converged constant values for each opening ratios are compared with the theoretical and experimental curves described above. These values agree closely with Henry's experimental curve. The contraction coefficients obtained in several scale models are shown in Fig.6 with Fangmeier – strelkoff's theoretical curve [2]. As done in the data of discharge coefficient, using the average values for channel widths, these data are re-drawn in Fig.7. In Fig.7, the experimental data by Benjamin is shown. From these two figures it is known that the scale effect in the contraction coefficients is similar to that of the discharge coefficients. That is, the coefficient becomes larger with the decrease of model size, and it seems that the scale effect is negligible in the model where the gate opening is over 6.0 cm. These results in contraction coefficients suggest that there is a close relationship between the scale effects in the contraction coefficients and the discharge coefficients. Benjamin presumed that the scale effect in the data of Fig.6 is related to the boundary layer growth on channel bottom. But, so far as author's measurement the boundary

layer thickness is very small, and it is not sufficient to explain the scale effect. Fig.8 shows the coefficients of energy loss  $k$  obtained in several scale models. The trend of the scale effects in this coefficient is the same as that in the other two coefficients. This fact means that the energy dissipation in effluxes is also related to the scale effect in the discharge coefficients closely, and that the role of viscosity is significant in the scale effect.

The surface profile and the downstream tail water depth  $Y_t$  were measured using point gauge. Because the water surface along the hydraulic jump fluctuates, it should be treated as an averaged depth. The surface profile measurements for all conditions are shown in Fig.9. For each experimental condition, detailed measurements along the centerline at the plane of  $z/B = 0.5$  were carried out to obtain vertical profiles of the flow characteristics. These characteristics include the time – averaged longitudinal component of velocity  $\bar{u}$  and vertical component  $v$ , kinematic turbulence shear stress –  $u'v'$  and turbulence intensities  $u'$  and  $v'$ . The number of measured sections for each run ranged from 10 to 14 depending on different experimental conditions. More sections were covered near the silled gate than downstream of the recirculating zone. As an example, the measurements are plotted from Fig. 10 to Fig. 14. It should be noticed that all the relationships are nondimensionalized by a length scale  $Y_1$  and a velocity scale  $U_1$ . For each section, extra measurements were made in vertical planes with  $z/B = 0.5$  and 0.25. Usually six carefully selected data points at both these planes were measured to check the spanwise variation of the flow. Besides these measurements, another set to indicate spanwise variation was taken for each section at the plane of  $y/Y_1 = \text{constant}$ . This  $y/Y_1$  was selected close to the surface and kept constant for each run. One example of the spanwise variation plot is shown in Fig. 15, where only the measurements for longitudinal velocity profiles are plotted. The original intension for these extra measurements was to validate the dimensionality of the flow as it was previously treated. The longitudinal velocity and turbulent shear stress profiles from these measurements are plotted in Fig. 16 and Fig. 17 respectively. From the flow development point of view a submerged jump could be divided into three distinguishable regions. These are the developing, the fully developed and the

recovering regions as shown in Fig. 1(b). The end of the potential core denotes the end of the developing region and the beginning of the fully developed region. If the length of the roller  $L_{rsj}$  is defined as the length of a submerged jump as in reference [16],  $L_{rsj}$  denotes the end of the fully developed region and the beginning of the recovering region. The developing region in a submerged jump is similar to that of a wall jet. One difference is that the flow near the gate in a submerged jump undergoes acceleration due to negative pressure gradient caused by falling water surface. Because this region limited to about 17% of  $L_{rsj}$ , the following discussion will concentrate on the fully developed region which occupies almost 80% of  $L_{rsj}$ . The flow in the fully developed region demonstrates some degree of similarity. Because the maximum vertical velocity  $v$  in the recirculating zone for all submerged jumps is only about 7% of  $U_1$ . Liu [26] reported that there were two distinguishable vortices on the water surface of a submerged jump at the corners of the gate, but how they influenced the flow was not clear. The present study shows not only the existence of such vortex motion but also its significance. As shown in Fig. 16 (a) the vortex motion near the gate extends from the water surface to the shear layer. Therefore, it is reasonable to expect that its influence will be significant under relatively high submergence. This vortex motion also alters the downstream flow development quite significantly. As shown in Fig. 16 (b) at  $x/Y_1 = 30$ , the maximum velocity ( $u_m$ ) near the center plane of the channel is about 25% smaller than that near the side wall. Further downstream at  $x/y_1 = 60$ , in which, it is near the end of the fully developed region, the difference between the maximum  $\bar{u}_m$  near the side wall and minimum  $\bar{u}_m$  near the center plane is up to 40% as shown in Fig. 16 (c). Another effect is that the length scale for  $u$  near the side wall is higher than that near the center plane. This phenomena is called the climb of a wall jet near the side wall by George [7] and Rajaratnam [17]. This climbing effect is believed due to the influence of this vortex motion. As shown in Fig. 16 (a) the flow close to the bed is two dimensional shortly after the inlet, but on top of this region there is vortex motion. This motion causes reversing flow near the center plane and forward flow near the side wall. As shown in Fig. 17, the shear stress near the center is about 46% higher than that near the side wall. Therefore, this

vortex motion causes faster diffusion near the centre plane than near the side wall at locations further downstream. The results are of course that  $\bar{u}_m$  near the center plane is smaller than that near the side wall.

## 7. CONCLUSIONS:

The following conclusions could be drawn from the present study of the scale effect in the efflux from an underflow gate and submerged hydraulic jumps in a rectangular channel.

The coefficient of discharge becomes larger as the model size becomes smaller at constant opening ratio  $Y/h_1$ . The scale effect in the coefficients obtained by the model which gate opening are larger than 6.0 cm seems to be very small for  $Y_1/h_1 < 0.5$ . The results show that there is a close relationship between the scale effects in the contraction and the discharge coefficients. The contraction coefficient becomes larger with the decrease of model sizes, and it seems that the scale effect is negligible in the model which where gate opening is over 6.0 cm. The energy dissipation in effluxes is also related to the scale effect in the discharge coefficients closely. Generally, the results reveals that the scale effect initiates when the gate opening becomes less than 6.0 cm, and that the degree of effects is notable at the larger value of the opening ratio. The scale effects in the contraction coefficient and in the coefficient of energy loss which are the main factors composing the discharge coefficient show the same trend as in the discharge coefficient.

Submerged hydraulic jumps are three dimensional in nature. The climbing effect of mean velocity component  $\bar{u}$  near side wall is due to the vortex motion near the gate. In the fully developed region of a submerged jump, which occupies about 80% of roller length  $L_{rsj}$ , the flow demonstrates some degree of similarity. The maximum turbulence quantities could be estimated from Froude number  $F_{r1}$  and submergence  $S$  and therefore the major flow characteristics can be determined. The maximum vertical velocity  $\bar{v}$  in the recirculating zone for all submerged jumps is only about 7% of  $U_1$ . Also, the results show that the maximum velocity  $\bar{u}_m$  near the center plane is smaller than that near the side wall. The turbulence shear stress  $-\overline{uv'}/U_1^2$  near the center is about 40% higher than that near the side wall. After the hydraulic jump the flow will recover into two dimensional flow. If a two

dimensional prediction for submerged jump is obtained, its limitations should be emphasized and its results should be interpreted properly.

### 8. NOMENCLATURE:

B : Channel width.

$\bar{u}$  : Streamwise mean velocity component in x-direction.

$u_{max}$ : Max. streamwise velocity component in x-direction.

$u'$  : Streamwise component of turbulence intensity in x-direction (RMS).

$\bar{v}$  : Vertical mean velocity component in y-direction.

$v'$  : Vertical component of turbulence intensity in y-direction (RMS).

$Fr_1$  : Inlet Froude number =  $U_1/\sqrt{gY_1}$ .

$Re_1$  : Inlet Reynolds number =  $U_1Y_1/\nu$ .

$U_1$  : Longitudinal velocity component at the inlet.

$\nu$  : Kinematic viscosity.

$We_1$  : Webber number.

x : Longitudinal axis along channel length.

y : Transverse axis along channel height.

z : Lateral axis along channel width.

g : Gravitational acceleration.

Q : Flow discharge.

$h_1$  : Water surface depth.

S : Submergence factor =  $(Y_1 - Y_2)/Y_2$ .

$L_{rsj}$  : Length of roller.

$Y_1$  : Inlet opening.

$Y_2$  : Sequent depth of a free jump.

$Y_1$  : Downstream depth.

### 9. REFERENCES:

- [1] Anwar, H.O., "Discharge Coefficient for Control Gates", J. Water Power, April, 1964, pp.152 - 159.
- [2] Benjamin, T.B., "On the Flow in Channels When Rigid Obstacles are placed in the Stream" Jour. Fluid Mech. 1, 1956, pp. 227 - 248.
- [3] El-Saiad, Atef A., Abdel, H.E., and Hammad, M.N., "Effect of Sill under Gate on the Discharge Coefficient", J. of the Egyptian Society of Engineers, Vol.30, No.2, 1991, pp. 13 - 16.
- [4] El-Saiad, Atef A., Abdel H.E., Owais, T.M. and Hammad, M.N., "Characteristics of Submerged Flow under Sluice Gate with Sill", Ain Shims Univ. Engg. Bulletin, Vol.26 No.1, March, Cairo, Egypt, 1991, pp. 109-120."
- [5] El - saiad, A., "Study of Submerged Flow characteristics under Silled Sluice Gates", M. Sc. Thesis Ain Shams Univ., Cairo, Egypt, 1990.
- [6] Frangmeier, D.D. and Strelkoff, T.S., "Solution for Gravity Flow under a Sluice Gate", J. EM - Div, Proc. ASCE (1968) 2, pp. 153 - 176.
- [7] George, A. R., "An Investigation of a Wall Jet in a Free Stream", Princeton University, Rept. No, 479, 1959.
- [8] Henry, H. Discussion of "Diffusion of Submerged Jets", Trans. Proc. ASCE, Vol. 115, 1950, pp. 687 - 697.
- [9] Henderson, F.M., "Open Channel Flow", Macmillan Publishing Co. Inc., New York, 1966, pp. 202 - 210.
- [10] Launder, B.E., and Rodi, W., "The Turbulent Wall Jets", Prog. Aerospace Sci., Vol. 19, 1981, pp. 81 - 128.
- [11] Mc Corquodale, J.A., "Hydraulic Jumps and Internal Flows", in Chapter 6, Encyclopedia of Fluid Mech., N.P. Chermisinoff ed., 1986, pp. 122 - 173.
- [12] Ohtsu, I. and Yasuda, Y., "Characteristics of Supercritical Flow Below Sluice Gate", J. Hydr. Engg. , Proc. ASCE, Vol. 120 , No. 3, March, 1994, pp. 332 - 346.
- [13] Rajaratnam, N. and Subramanya, K., "Flow Equation for the Sluice Gate", J. of Irrigation and Drainage Division, Proc. ASCE, Vol. 93, No. Hy4, July, 1967, pp. 167 - 186.
- [14] Rajaratnam, N., "Free Flow Immediately Below Sluice Gates", J. Hydraulics Division, Proc. ASCE, Vol. 103, No. Hy4, April, 1977, pp. 345 - 351.
- [15] Rayaratnam, N. and Subramanya, K., "Flow Immediately Below Submerged Sluice Gate", J. of Hydr. Divison, Proc. ASCE, Vol. 93, No.Hy4, July, 1977, pp. 57 - 77.

- [16] Rajaratnam, N., "Hydraulic Jumps", in *Advances in Hydrosience*, V.T. Chow, Ed. 4, Academic Press, New York, NY, 1967, pp. 198 - 280.
- [17] Rajaratnam, N., Discussion on "Pressure Fluctuations in Submerged Jump", by S. Narasimhan and V.P. Bhargava, *J. of Hydr. Division, ASCE*, 102 : HY12, 1976, pp. 1785 - 1787.
- [19] Resch, F.J. and Leathusser, H.J., "Reynolds Stress Measurements in Hydraulic Jumps", *J. of Hydr. Research, IAHR*, 10 : 4, 1972, pp. 409 - 430.
- [20] Rouse, J., Siao, T.T. and Nagaratnam, R. "Turbulence Characteristics of the Hydraulic Jump", *J. of Hydr. Division, ASCE*, 84 : HY1, Paper 1528, 1958.
- [21] Ranja Raju, K.G. and Visavadia, D.S., "Discharge Characteristics of a Sluice Gate Located on a Raised Crest", *Proc. IMEKO in Industry, Tokyo, Japan, Nov., 1997*, pp. 39 - 43.
- [22] Ranja Raju, K.G. "Flow through Open Channels", Tata Mc Graw Hill Publishing Company Limited, 1981, pp. 246 - 247.
- [23] Salama, M., "Flow Below Sluice Gate with Sill", *J. of Egyptian Society of Engineers*, Vol. 26, No. 4, 1987, pp. 31 - 36.
- [24] Talaat, A.M., "Note on Rating Sluice Gates" *Engg. Bulletin, Faculty of Engg., Ain Shams Univ., No. 22, Vol. 1, 1988*, pp. 92 - 109.
- [25] Wilson, D.J. and Goldstein, R.J., "Turbulence Wall jets with Cylindrical Streamwise Surface Curvature", *J. of Fluids Engg., Trans. ASCE*, Vol. 98, 1976, pp. 550 - 557.
- [26] Liu, H.K., "Diffusion of Flow from a Submerged Sluice Gate, Thesis Presented to the State Univ. of Iowa, Iowa, in Partial Fulfillment of the Requirements for the Degree of Master of Science



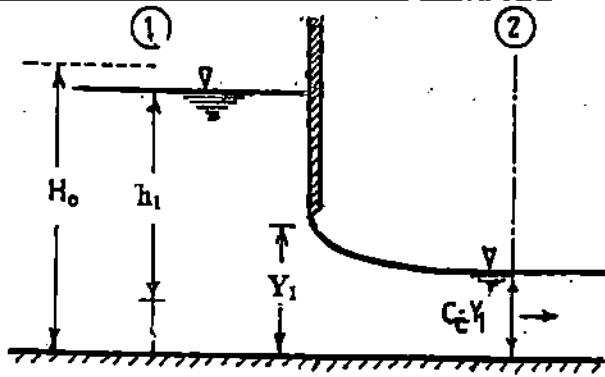


Fig. 1 (a) Free efflux from an underflow gate.

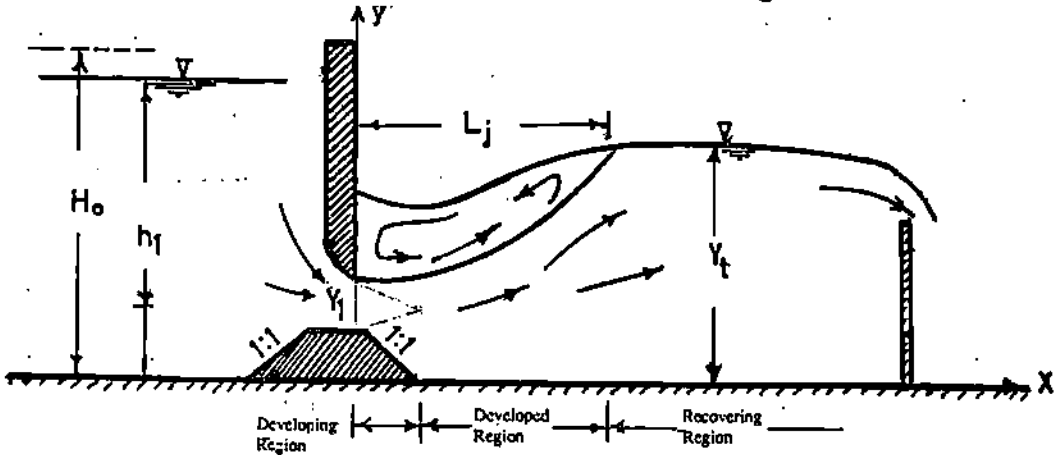


Fig.1 (b) Definition sketch for free and submerged flow below sluice gate with sill.

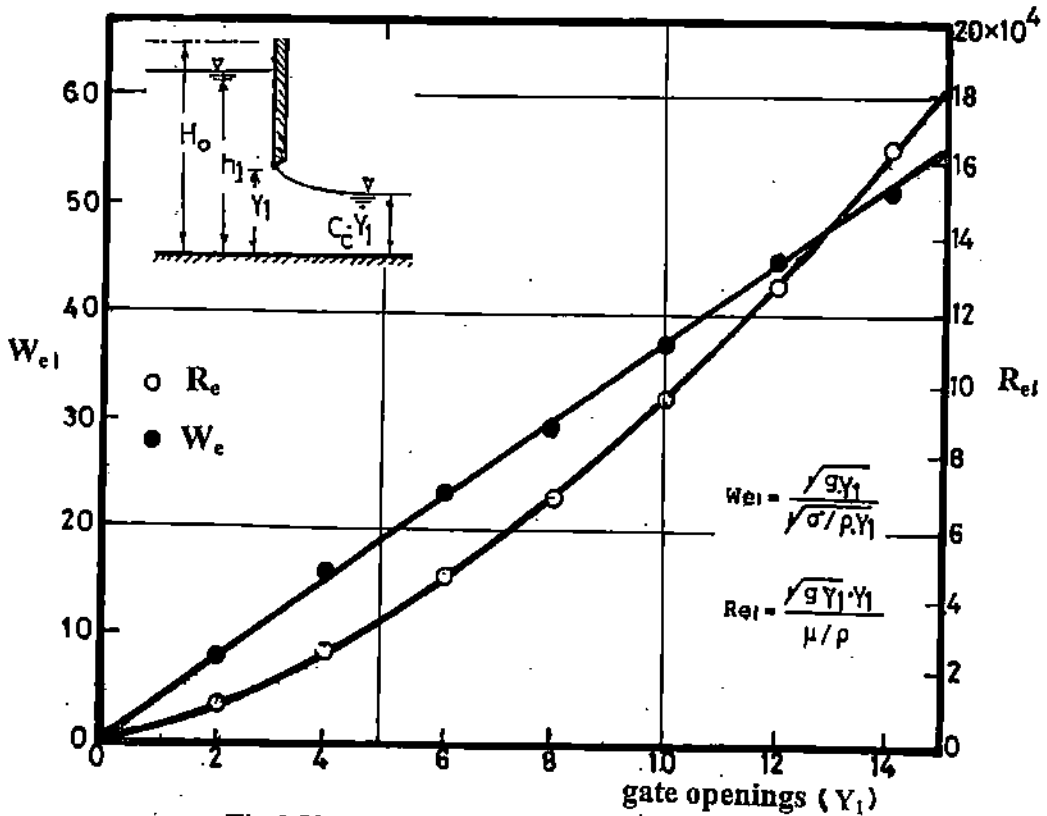


Fig.2 Variation of  $R_e$  and  $W_e$  to gate openings.

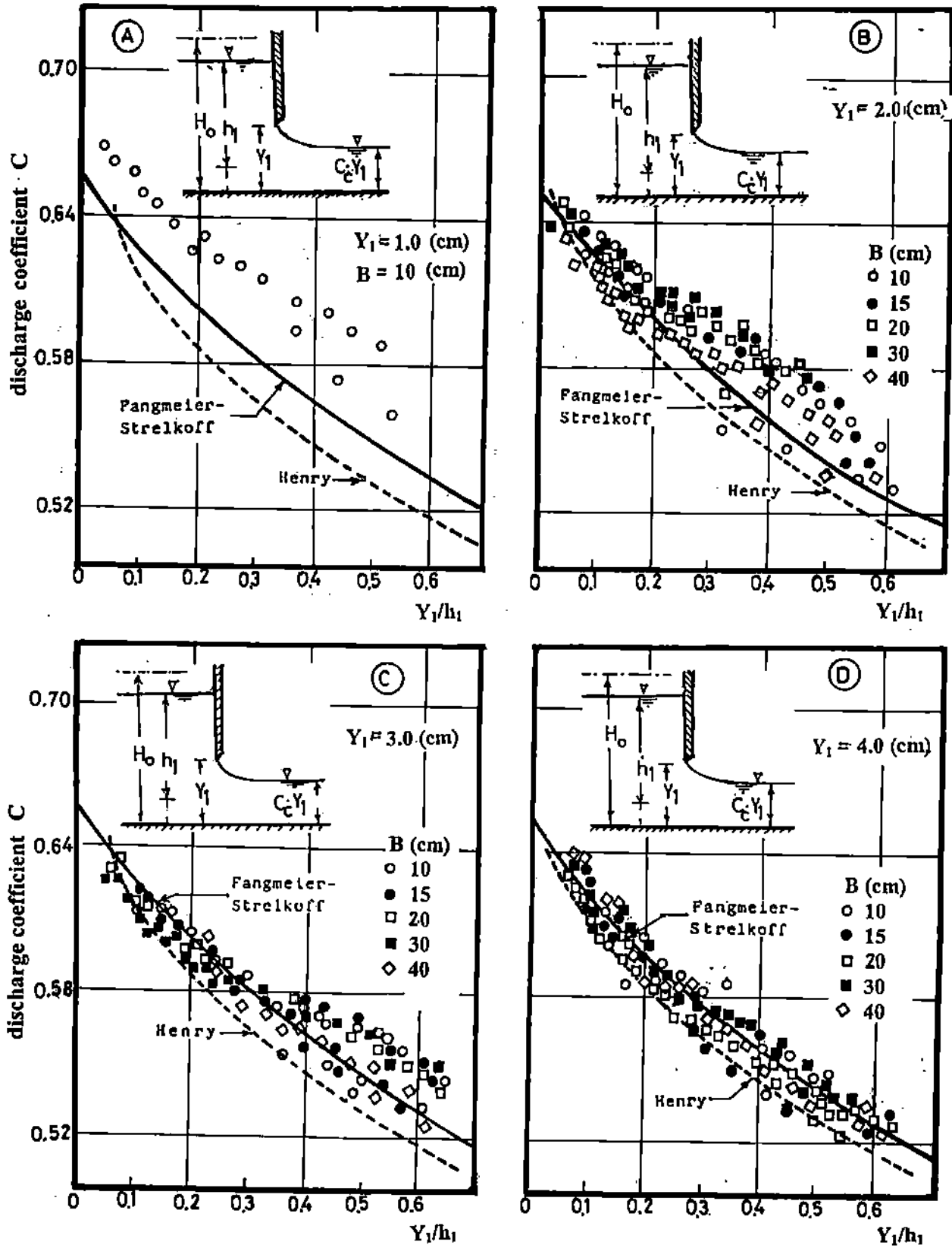


Fig.3 Continue

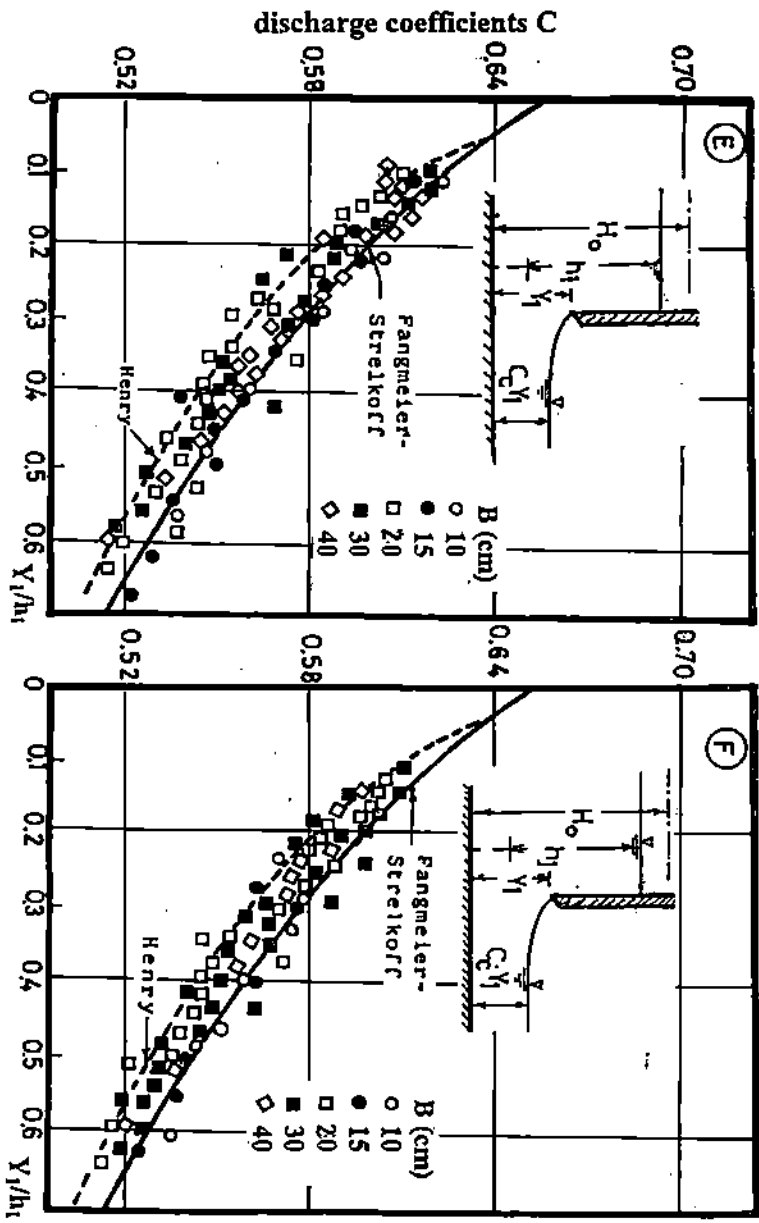


Fig.3 Variation of discharge coefficients C with opening ratio  $Y_1/h_1$  for different gate width B at different  $Y_1$ .

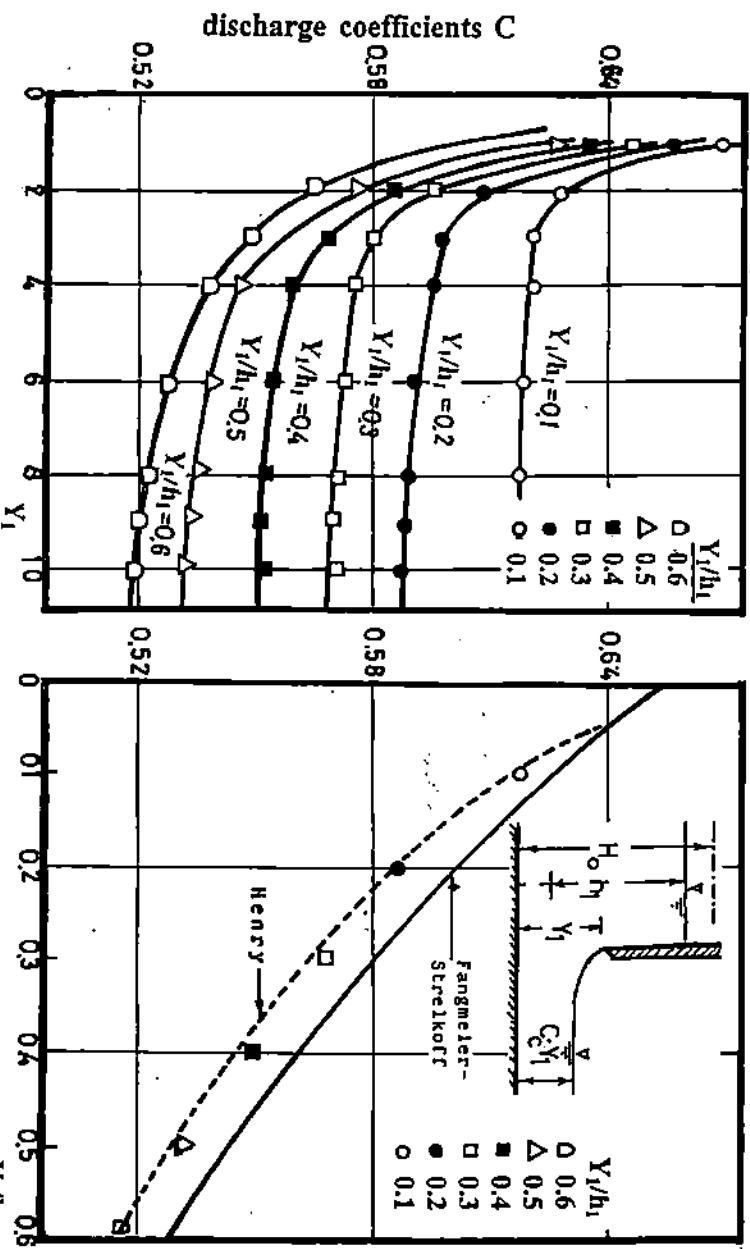


Fig.4 Scale effect in discharge coefficients C.

Fig.5 Discharge coefficients without scale effect.

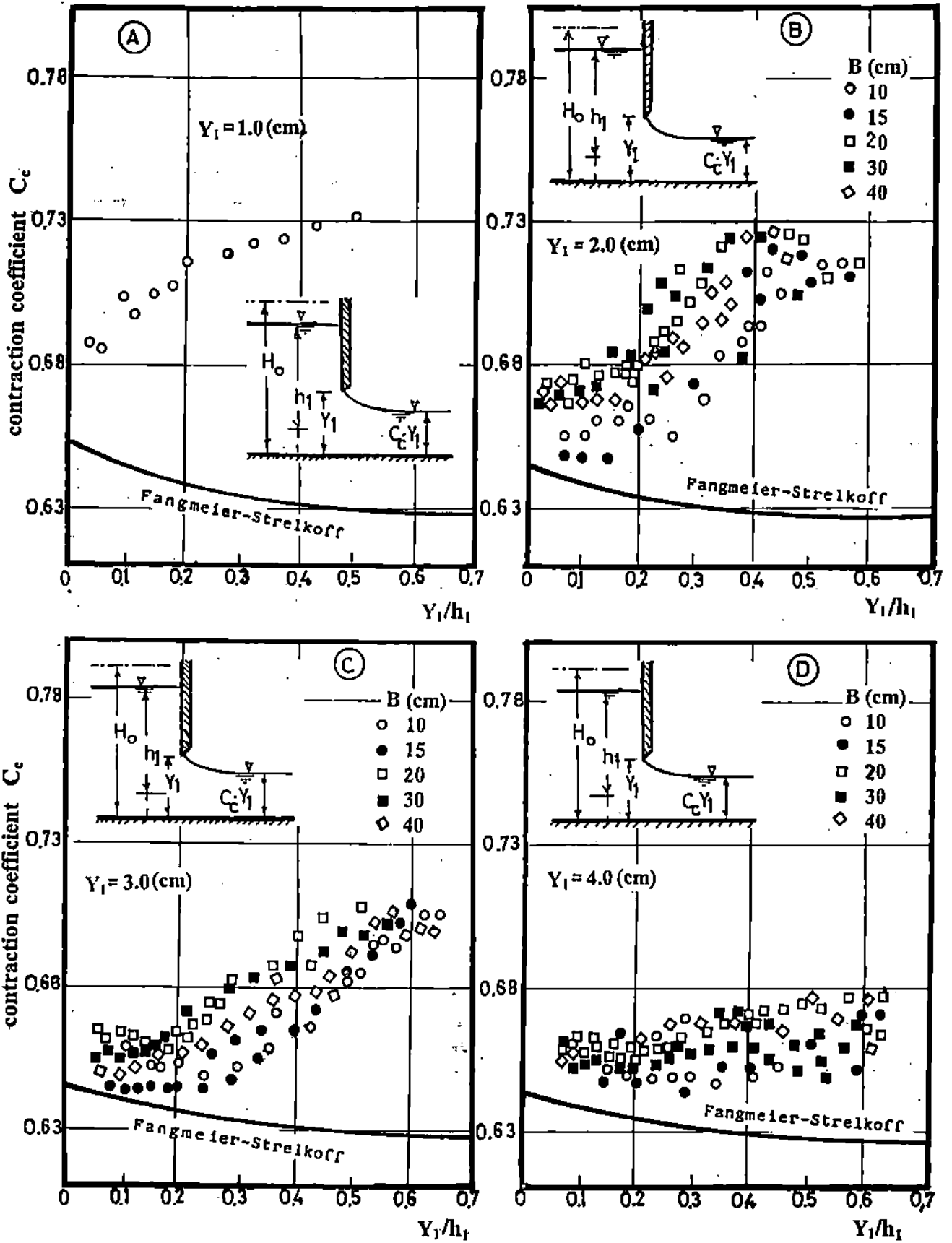


Fig.6 Continue

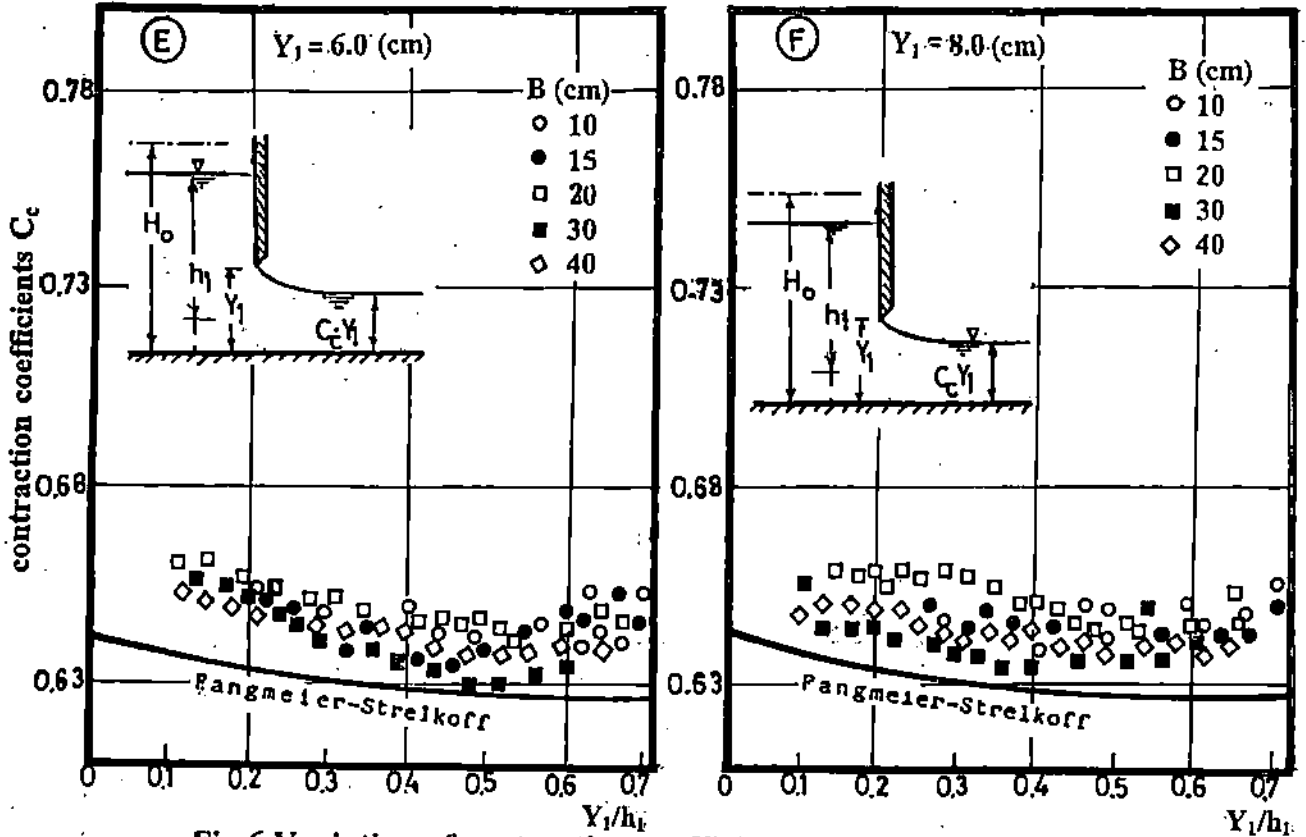


Fig.6 Variation of contraction coefficients  $C_c$  with opening ratio  $Y_1/h_1$  for different gate width  $B$  at different  $Y_1$ .

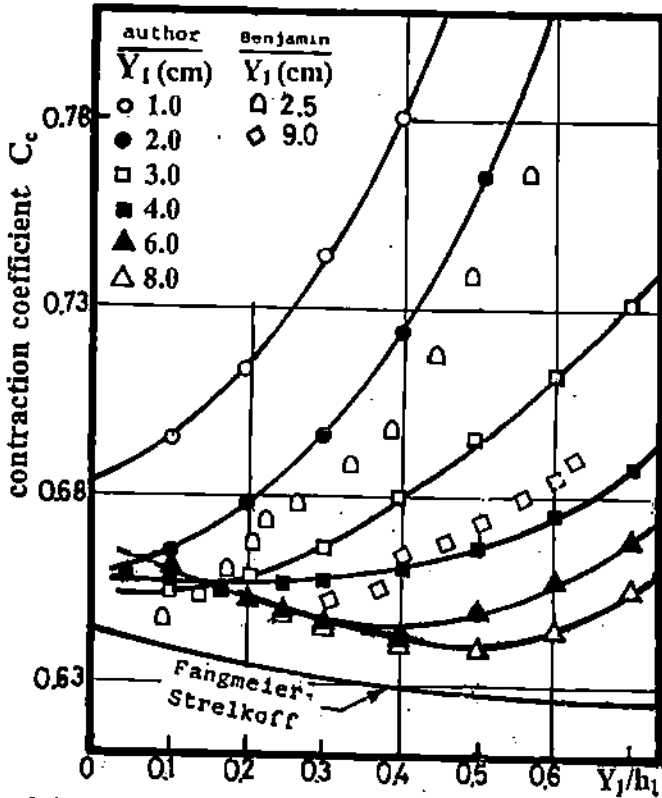


Fig.7 Variation of contraction coefficients  $C_c$  with opening ratio  $Y_1/h_1$  for different gate opening  $Y_1$ .

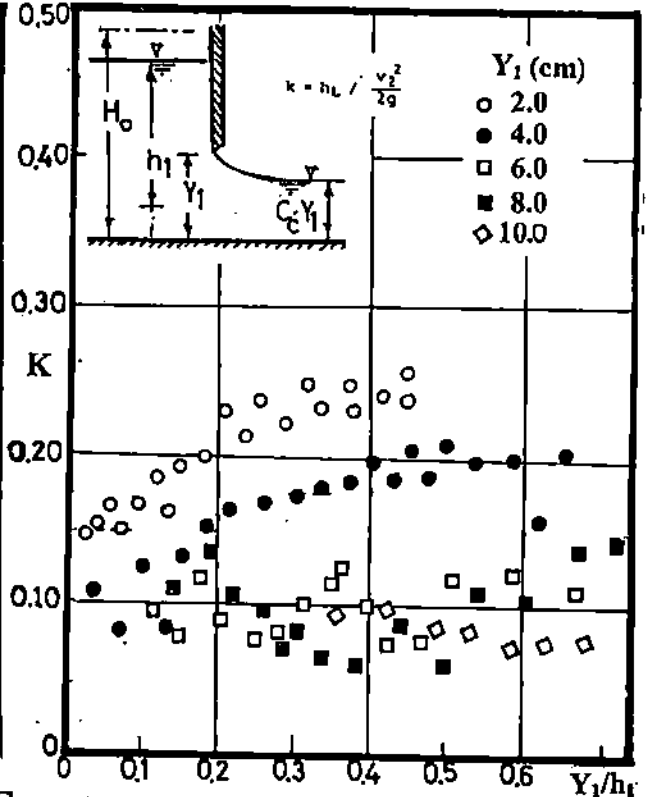


Fig.8 Variation of coefficient of energy loss  $K$  with opening ratio  $Y_1/h_1$  for different gate opening  $Y_1$ .

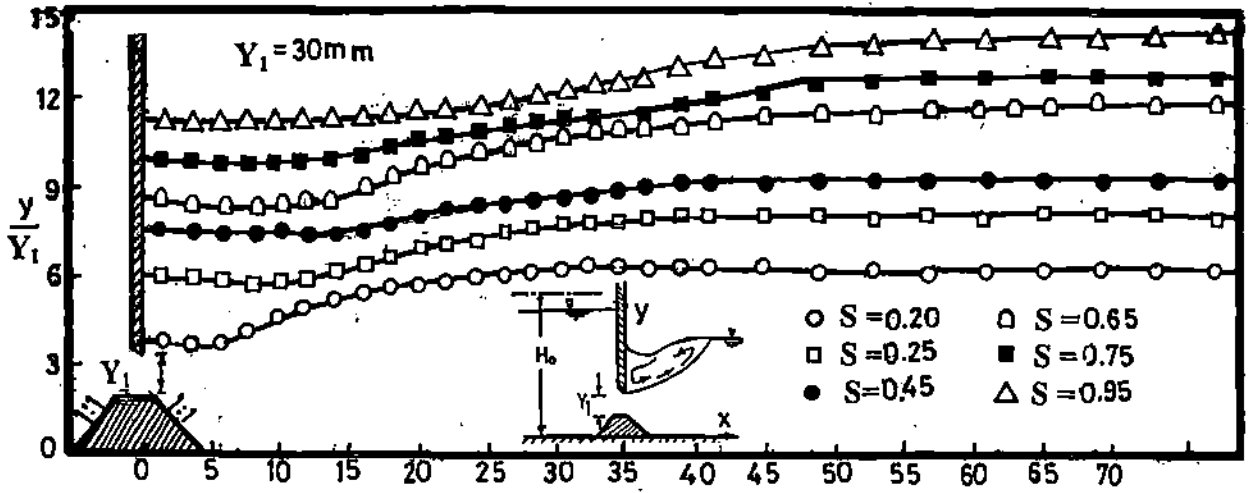


Fig.9 Variation of water surface profile for different submergence factor  $S$ .

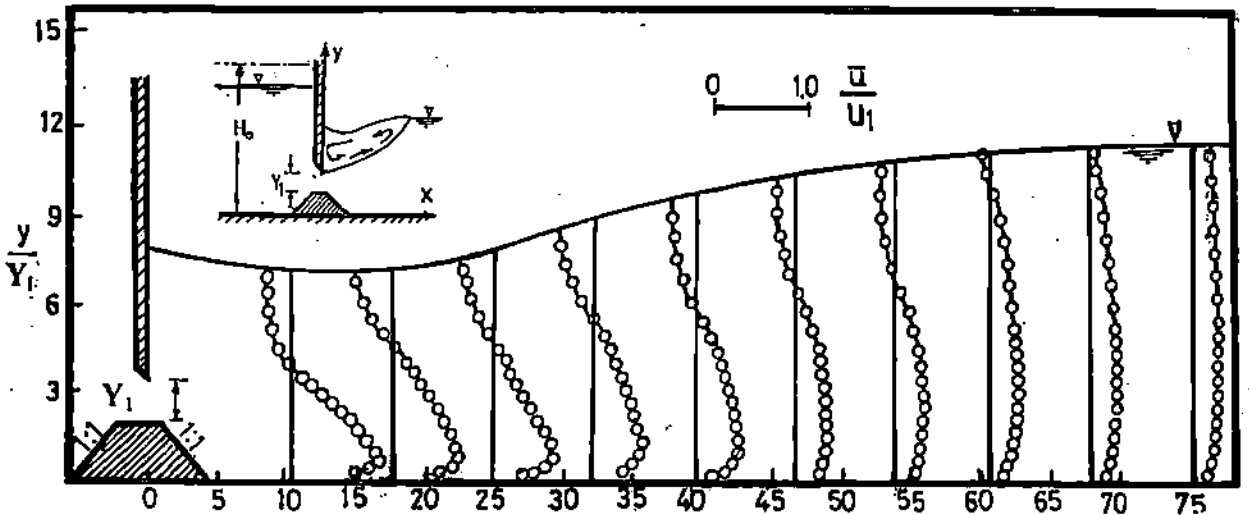


Fig. 10 Variation of streamwise mean velocity  $\bar{u} / U_1$  along the depth at different cross sections ( $F_1=8, S=0.25$  and  $z/B=0.5$ ).

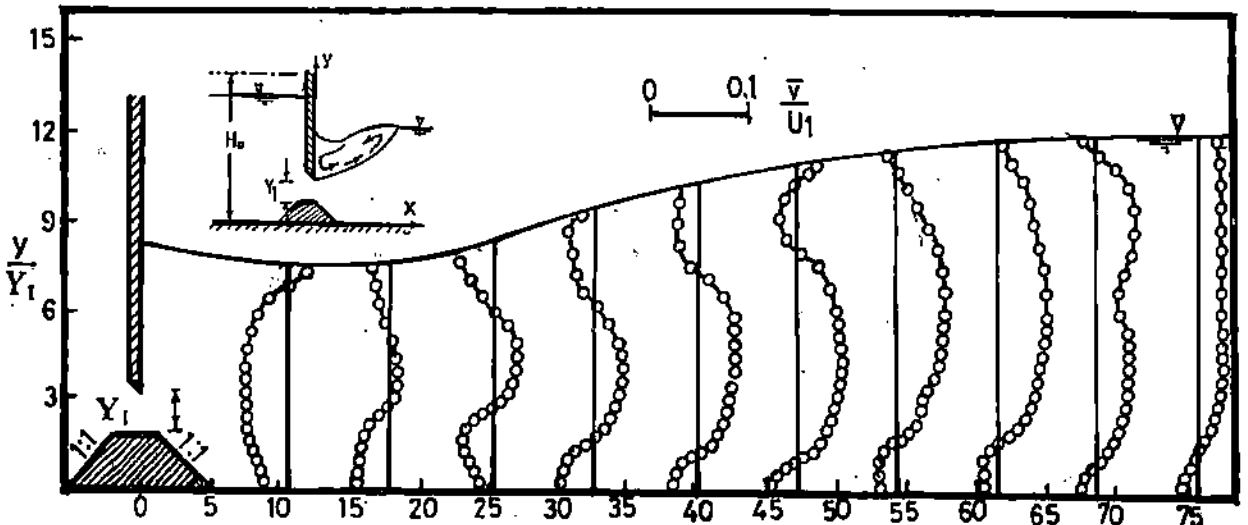


Fig.11 Variation of vertical mean velocity  $\bar{v} / U_1$  along the depth at different cross sections ( $F_1=8, S=0.25$  and  $z/B=0.5$ ).

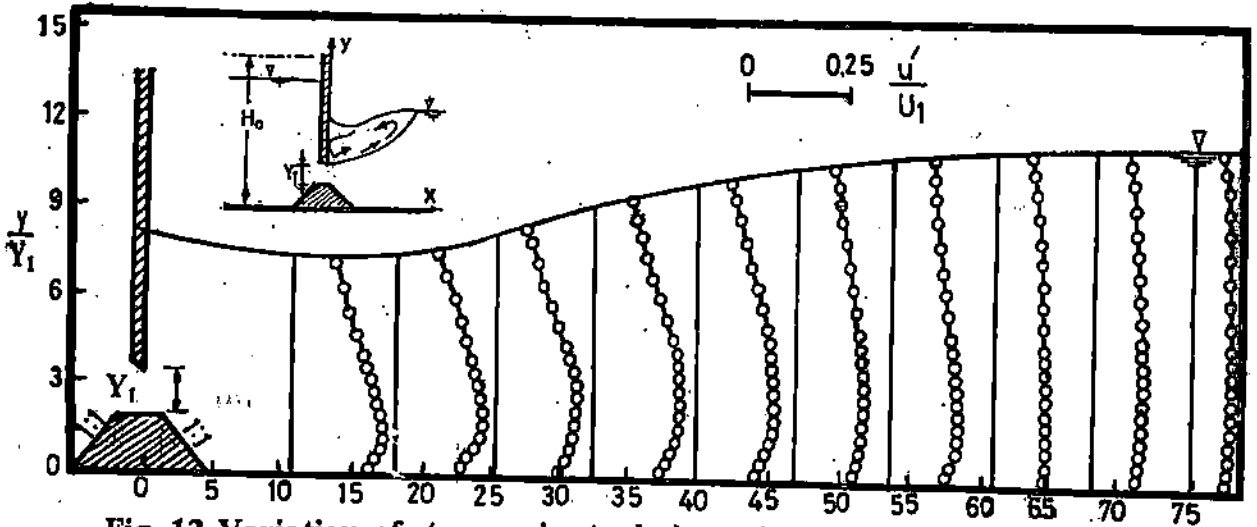


Fig. 12 Variation of streamwise turbulence intensity  $\bar{u}' / U_1$  along the depth at different cross sections ( $F_1=8$ ,  $S=0.25$  and  $z/B=0.5$ ).

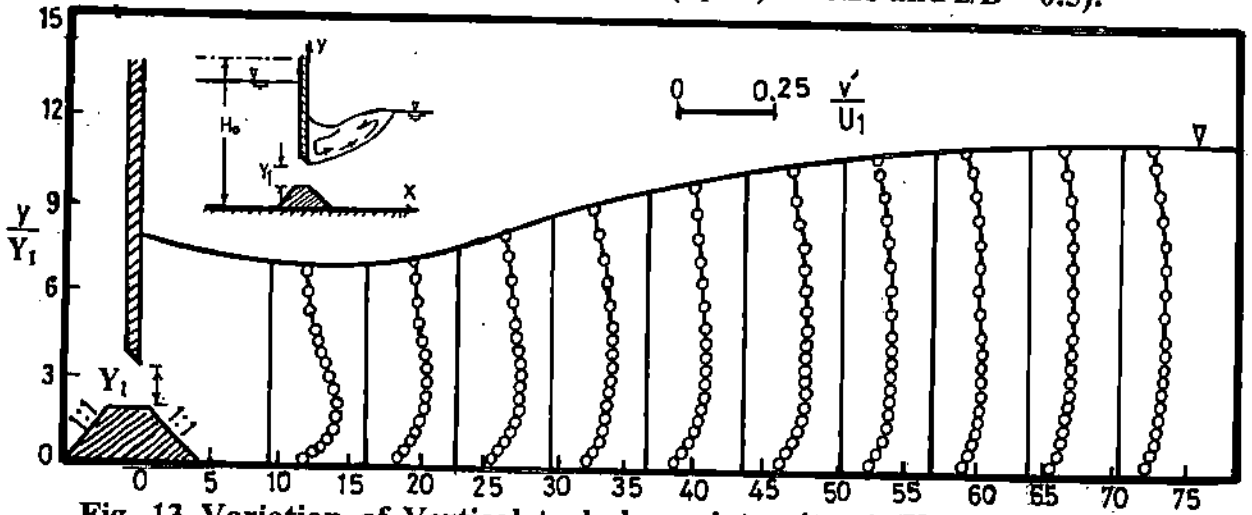


Fig. 13 Variation of Vertical turbulence intensity  $\bar{v}' / U_1$  along the depth at different cross sections ( $F_1=8$ ,  $S=0.25$  and  $z/B=0.5$ ).

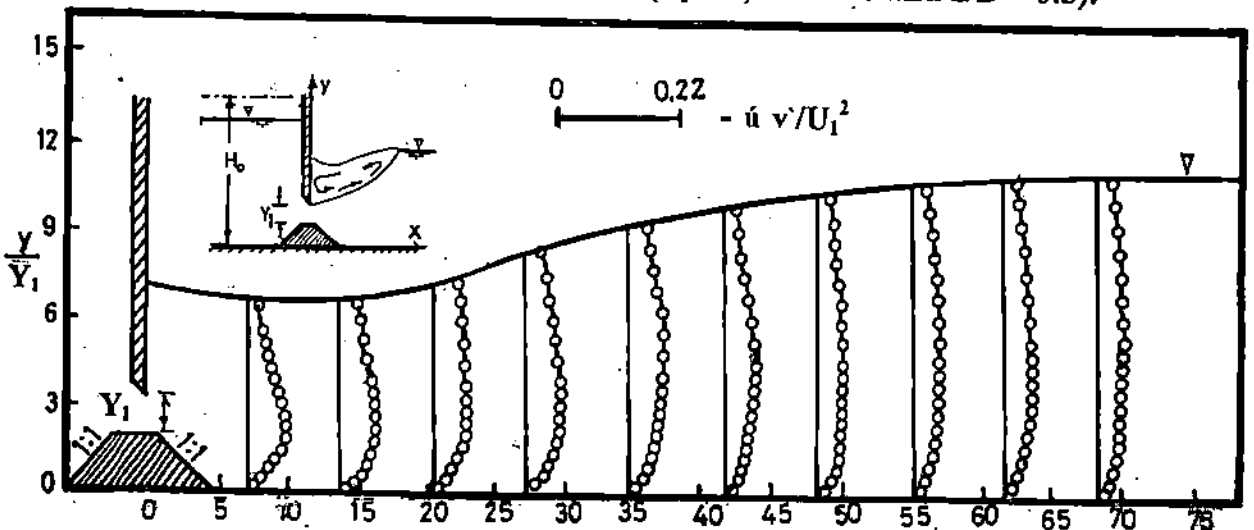


Fig. 14 Variation of turbulence shear stress  $-\bar{u}' v' / U_1^2$  along the depth at different cross sections ( $F_1=8$ ,  $S=0.25$  and  $z/B=0.5$ ).

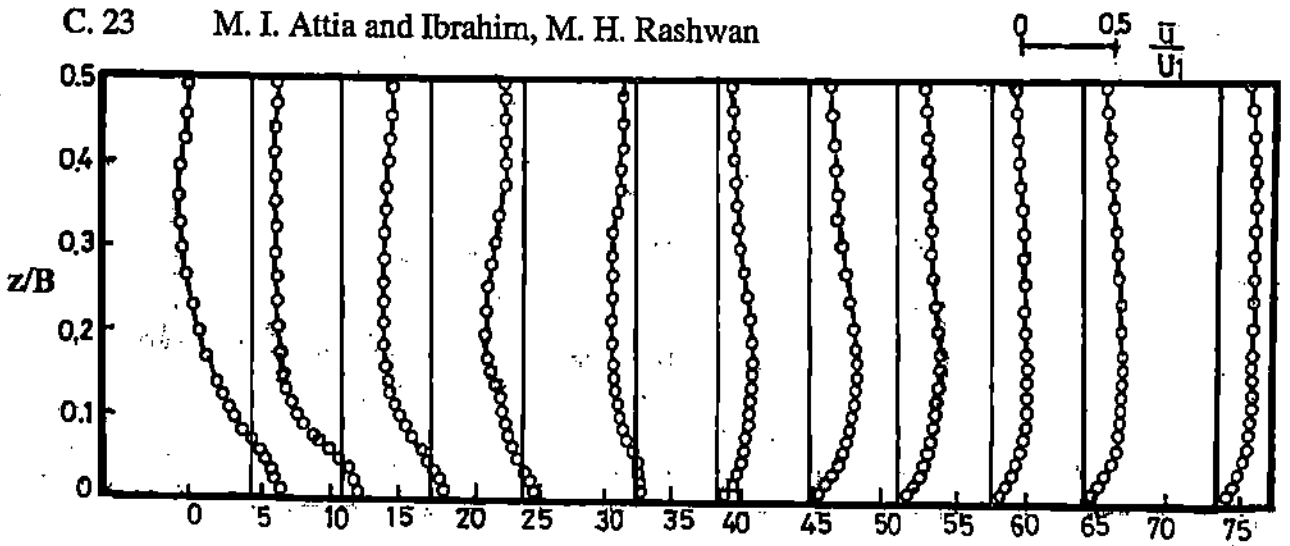


Fig. 15 Variation of streamwise mean velocity  $u/U_1$  at the plane of  $y/y_1 = 5$  ( $F_1 = 8$  and  $S = 0.25$ )

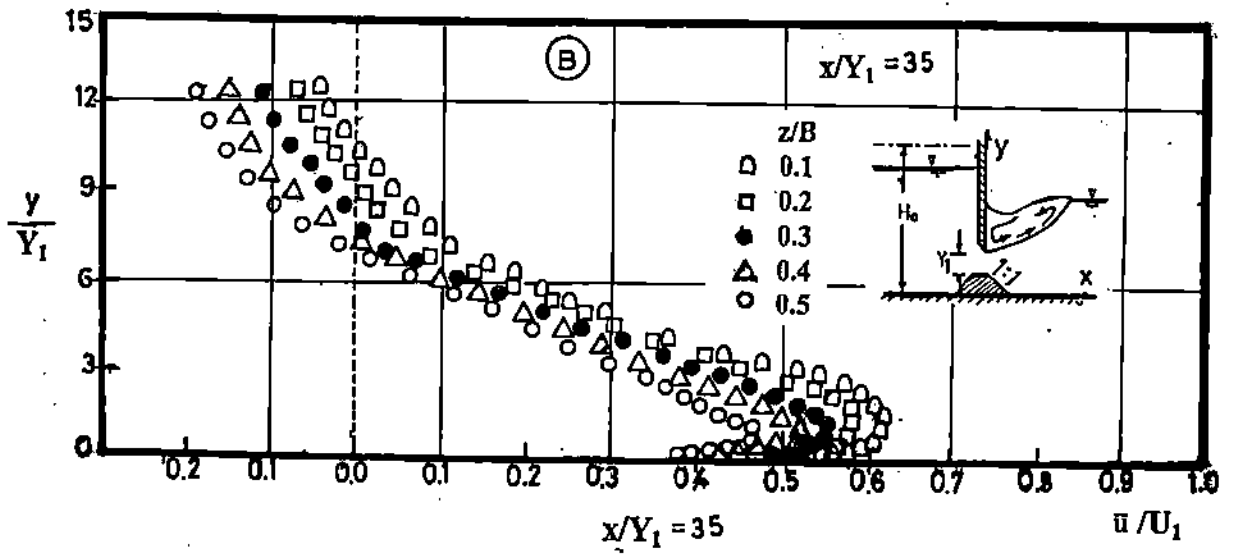
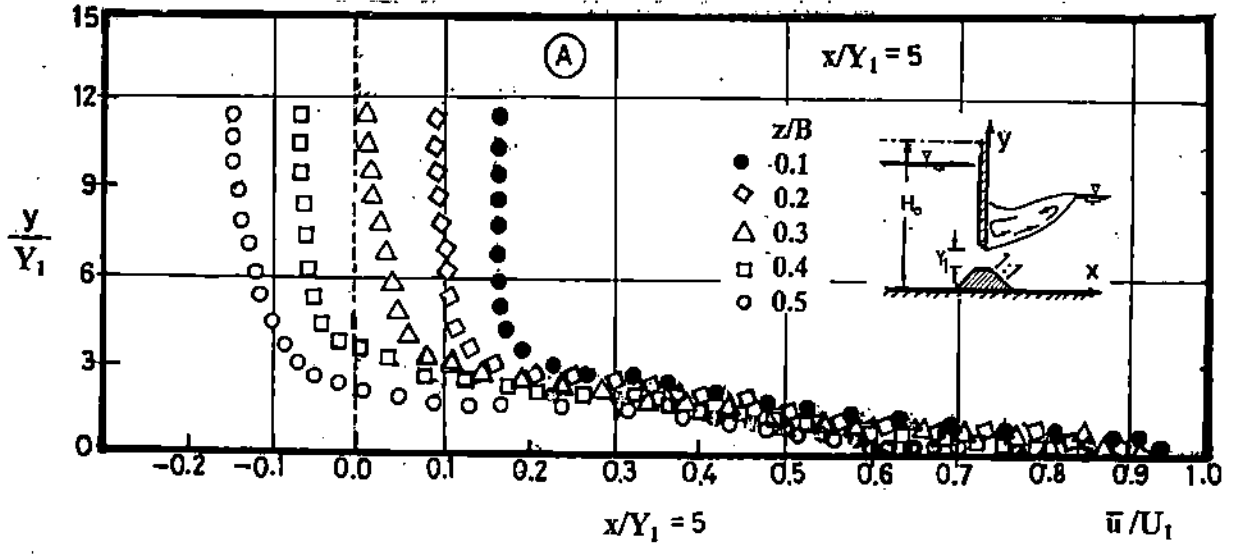


Fig. 16 (a), (b) Continue



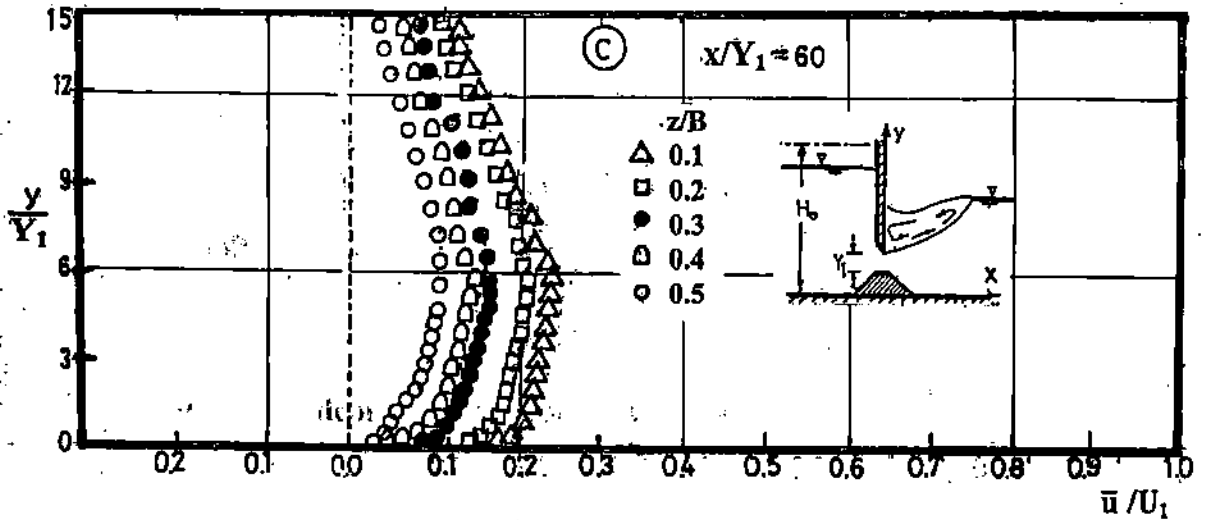


Fig. 16 (a) , (b) and (c) Variation of streamwise mean velocity  $\bar{u}/U_1$  along the depth for different  $z/B$  ( $F_1=5$  and  $S=0.25$ )

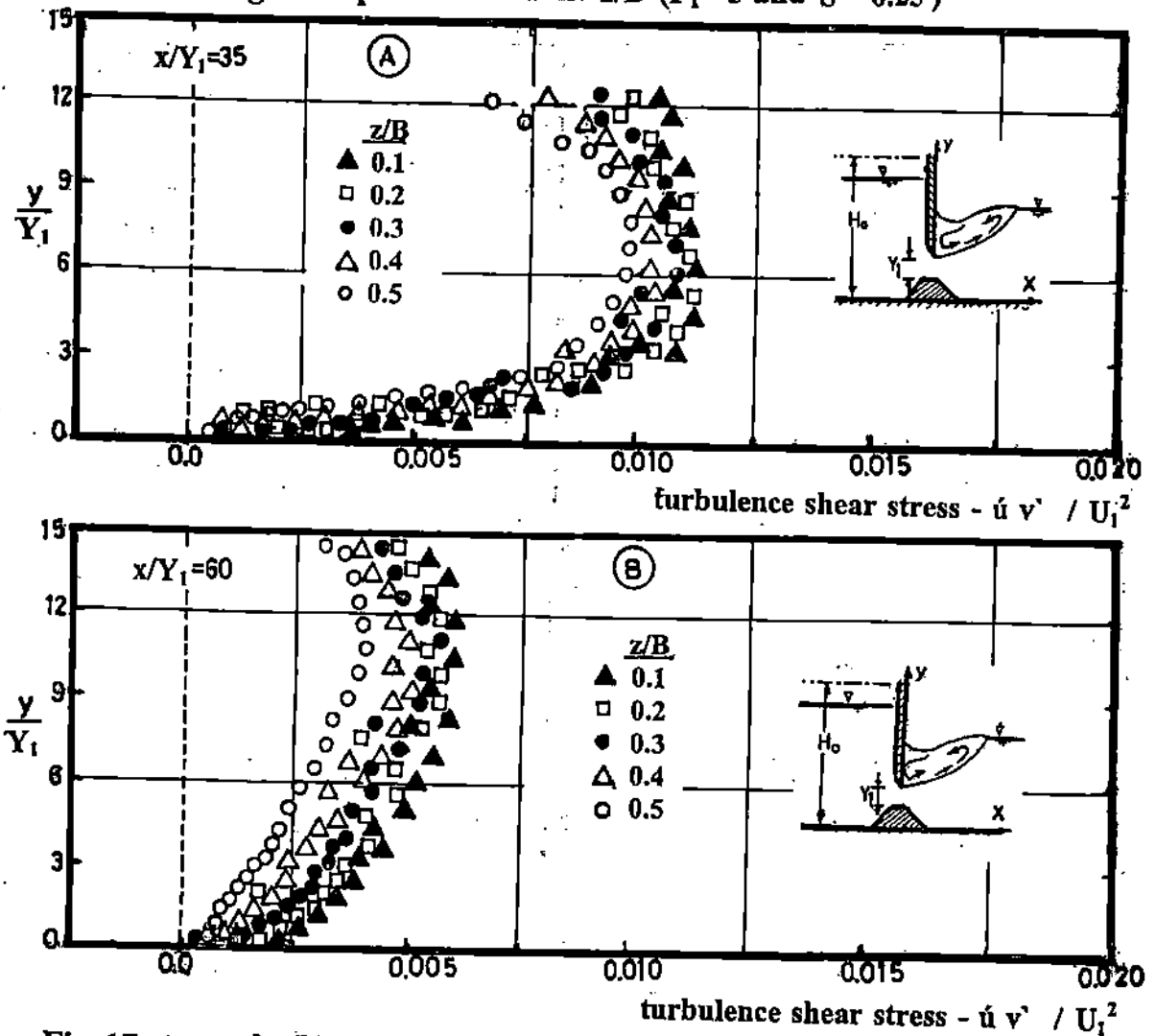


Fig. 17 (a) and (b) Variation of turbulence shear stress  $-\bar{u}'v'/U_1^2$  along the depth for different  $x/Y_1$  at different  $z/B$  ( $F_1 = 5$  and  $S = 0.6$ )